Human Skeletal Muscle Cells With a Slow Adhesion Rate After Isolation and an Enhanced Stress Resistance Improve Function of Ischemic Hearts

Masaho Okada[1,2], Thomas R Payne[1–4], Lauren Drowley[1,2], Ron J Jankowski[4], Nobuo Momoi[5], Sarah Beckman[1], William CW Chen[1,3], Bradley B Keller[5], Kimimasa Tobita[5] and Johnny Huard[1–3,6]

[1]Stem Cell Research Center, Children's Hospital of Pittsburgh, Pittsburgh, Pennsylvania, USA; [2]Department of Orthopaedic Surgery, University of Pittsburgh, Pittsburgh, Pennsylvania, USA; [3]Department of Bioengineering, University of Pittsburgh, Pittsburgh, Pennsylvania, USA; [4]Cook Myosite, Pittsburgh, Pennsylvania, USA; [5]Department of Pediatrics, Children's Hospital of Pittsburgh, Pittsburgh, Pennsylvania, USA; [6]Department of Molecular Genetics and Biochemistry, University of Pittsburgh, Pittsburgh, Pennsylvania, USA

Identification of cells that are endowed with maximum potency could be critical for the clinical success of cell-based therapies. We investigated whether cells with an enhanced efficacy for cardiac cell therapy could be enriched from adult human skeletal muscle on the basis of their adhesion properties to tissue culture flasks following tissue dissociation. Cells that adhered slowly displayed greater myogenic purity and more readily differentiated into myotubes *in vitro* than rapidly adhering cells (RACs). The slowly adhering cell (SAC) population also survived better than the RAC population in kinetic *in vitro* assays that simulate conditions of oxidative and inflammatory stress. When evaluated for the treatment of a myocardial infarction (MI), intramyocardial injection of the SACs more effectively improved echocardiographic indexes of left ventricular (LV) remodeling and contractility than the transplantation of the RACs. Immunohistological analysis revealed that hearts injected with SACs displayed a reduction in myocardial fibrosis and an increase in infarct vascularization, donor cell proliferation, and endogenous cardiomyocyte survival and proliferation in comparison with the RAC-treated hearts. In conclusion, these results suggest that adult human skeletal muscle-derived cells are inherently heterogeneous with regard to their efficacy for enhancing cardiac function after cardiac implantation, with SACs outperforming RACs.

Received 4 November 2010; accepted 21 September 2011; published online 8 November 2011. doi:10.1038/mt.2011.229

INTRODUCTION

Skeletal muscle is an attractive source of progenitor cells for autologous cell therapy due to its abundance and accessibility. Progenitor cells in skeletal muscle, generally referred to as myoblasts (or satellite cells), are numerous and heterogeneous in nature.[1] The potential use of myoblasts for treating muscle disorders has been hindered, at least in part, by high rates of cell death after transplantation.[2–4] Recently, there has been interest in the identification and purification of populations of skeletal muscle-derived cells with the greater potential for cell-based therapies.[1,2,4–16]

We and others have used the preplate isolation technique to fractionate skeletal muscle progenitor cells from rodent skeletal muscle on the basis of selective adhesion characteristics to tissue culture flasks.[17] Isolating cells with this method yields cell populations that are classified by a rapid or slow adherence to the culture flask. Skeletal myoblasts derived from the rapidly adhering cell (RAC) fraction of rodent skeletal muscle were poor at muscle regeneration when transplanted into both skeletal and cardiac muscles.[14–16] In contrast, murine skeletal muscle-derived stem cells (MDSC) derived from the slowly adhering cell (SAC) fraction demonstrated a significant improvement in skeletal muscle regeneration in comparison with the rapidly adhering myoblast population.[14,15] In addition, after intramyocardial injection into a murine model of an acute myocardial infarction (MI), hearts transplanted with MDSCs demonstrated a greater improvement in cardiac function in comparison with hearts transplanted with myoblasts.[16] The mechanisms underlying the functional difference between MDSC and myoblasts were attributed to the ability of the MDSCs to survive and engraft significantly better than the myoblasts.[16] The survival of MDSCs may have led to improvements in the attenuation of adverse remodeling and capillary density throughout the infarcted tissue. These effects were presumably mediated through long-term secretion of factors by the engrafted MDSCs, since differentiation into *de novo* cardiomyocytes was an extremely rare occurrence.[16] Although these promising results were observed with rodent skeletal muscle, it remained to be determined whether RAC and SAC isolated from human skeletal muscle would produce similar outcomes after cell transplantation into the heart.

Here, we isolated and characterized RAC and SAC from human skeletal muscle. The efficacy of both populations was evaluated in an MI model using immunodeficient mice. Our results indicate that the slowly adhering fraction of human skeletal muscle-derived cells more effectively improved cardiac function when compared with the rapidly adhering fraction. The SAC also demonstrated greater survival under conditions of oxidative and inflammatory conditions of stress *in vitro* when compared with the RAC.

Correspondence: *Johnny Huard, 450 Technology Drive, 2 Bridgeside Point, Suite 206, Pittsburgh, Pennsylvania 15219, USA. E-mail: jhuard@pitt.edu*

RESULTS

Myogenic purity of RAC and SAC populations

Each cell population was analyzed for myogenic purity as determined by CD56 flow cytometry analysis. SAC populations contained a higher percentage of CD56-expressing cells when compared with the RAC populations (**Figure 1a**, SAC 83 ± 3% CD56-positive, RAC 39 ± 17%, $n = 3$ populations per group, $P = 0.07$).

Myogenic gene expression profiles

Evaluation of myogenic lineage genes in both the RAC and SAC populations demonstrated substantial expression of the myogenic cell markers desmin (*DES*) and m-cadherin (*CDH15*) as well as the myogenic determination gene *MYOD1* and the myogenic regulatory factor *MYF5* relative to the endogenous control gene *IPO8* (**Figure 1b**, average values of $n = 3$ donors). A modest expression of the *PAX7* transcription factor, which regulates the myogenic differentiation of satellite cells, was also detected (**Figure 1b**). Very low expression of the early satellite cell marker *PAX3* and the myogenic regulatory factors myogenin (*MYOG*) and *MYF6*, which are both involved in the specification of skeletal myoblasts into terminally differentiated myotubes, was observed (**Figure 1b**). As expected, a very low level of the skeletal muscle myosin heavy chain 2 (*MYH2*) gene, which is specifically expressed by terminally-differentiated skeletal myotubes, was detected in both populations, confirming that the RAC and SAC populations did not undergo terminal differentiation during expansion under normal culture conditions (**Figure 1b**). Of the myogenic genes expressed by both cell populations, the SAC populations demonstrated increased expression of the following myogenic lineage genes relative to the RAC populations: *DES* (SAC: 1.6 ± 0.4 relative to RAC, $n = 3$ donors, $P = 0.218$), *CDH15* (1.4 ± 0.5, $P = 0.454$), *PAX7* (3.5 ± 1.1, $P = 0.082$), *MYOD1* (2.0 ± 0.4, $P = 0.066$), and *MYF5* genes (1.7 ± 0.3, $P = 0.108$) (**Figure 1c**). These findings correlate with the higher levels of myogenic purity observed in the SAC populations in comparison with the RAC populations (**Figure 1a**).

The presence of other cell types in the RAC and SAC populations that could have been co-isolated from human skeletal muscle was evaluated based on the expression levels of lineage-specific genes. We observed undetectable or minimal expression of the endothelial cell-specific gene von Willebrand factor (*VWF*), the smooth muscle cell lineage gene calponin 1 (*CNN1*), the adipocyte-expressed gene glycerol-3-phosphate dehydrogenase 1 (*GPD1*), the preadipocyte gene delta-like homolog (*DLK1*, alias *PREF1*, and the pan-hematopoietic gene protein tyrosine phosphatase receptor type C (*PTPRC*, alias *CD45*) (**Figure 1d**). The SAC populations also displayed lower expression relative to the RAC populations of the extracellular matrix genes fibronectin (*FN1*, 0.53 ± 0.15 quantity relative to RAC, $P < 0.05$) and collagen type IV (*COL4A1*, 0.54 ± 0.11, $P < 0.05$) (**Figure 1e**), which are highly expressed by fibroblasts.[18] Taken together, these results suggest that the nonmyogenic cells ($CD56^-$) within the RAC and SAC populations were fibroblasts, as expected.

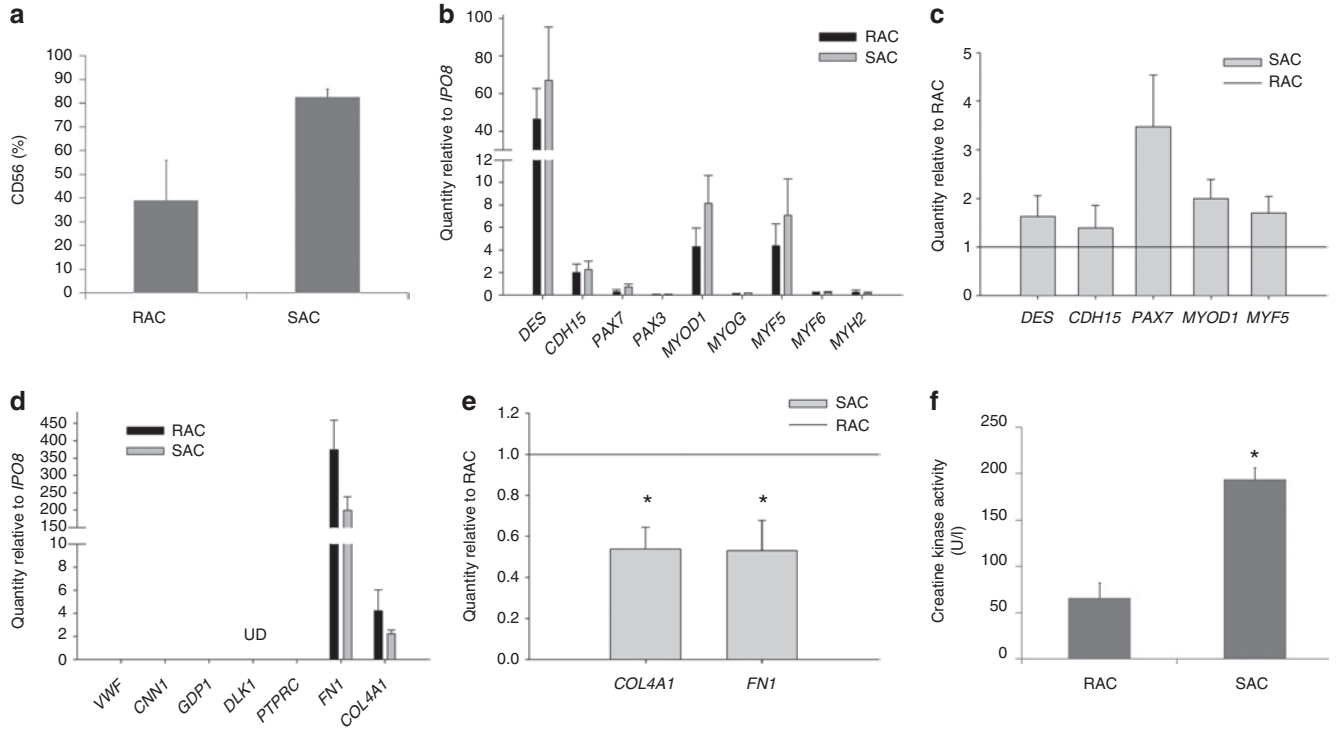

Figure 1 Characterization of the RAC and SAC after culture expansion. (**a**) Each cell population was analyzed for myogenic purity by CD56 flow cytometry. (**b**) Myogenic gene expression profiles were measured in the RAC and SAC populations. Gene expression values are relative to the endogenous control gene *IPO8*. (**c**) SAC populations demonstrated increased expression of all expressed myogenic genes relative to the RAC populations. (**d**) Detection of other cell types within the RAC and SAC populations: *VWF* for endothelial cells, *CNN1* for smooth muscle cells, *GPD1* for adipocytes, *DLK1* for preadipocytes (UD, undetectable), *PTPRC* for blood cells, and *FN1* and *COL4A1* for fibroblasts. (**e**) SAC populations displayed decreased expression of *FN1* and *COL4A1* relative to the RAC populations (*$P < 0.05$). (**f**) SAC populations more rapidly differentiated into multi-nucleated myotubes than the RAC populations as signified by increased creatine kinase activity (*$P < 0.05$). RAC, rapidly adhering cell; SAC, slowly adhering cell.

Myogenic differentiation

The myogenic differentiation potential of RAC and SAC was measured *in vitro* by creatine kinase activity, an enzyme expressed in differentiated myogenic cells. When subjected to culture conditions that support terminal differentiation, the SAC populations displayed higher creatine kinase activity values when compared with the RAC populations, indicating that SAC more rapidly differentiated into skeletal myotubes than RAC (**Figure 1f**, SAC 194 ± 13 units/liter, RAC 66 ± 16, $n = 3$ populations per group, $P < 0.05$).

Expression of paracrine factors

Under normal culture conditions, RAC and SAC highly expressed vascular endothelial growth factor A (*VEGFA*) and transforming growth factor-β1 (*TGFβ1*) genes. At lower levels, RAC and SAC populations also expressed fibroblast growth factor 2 (*FGF2*), platelet-derived growth factor-β (*PDGF*β), angiopoietin 1 (*ANGPT1*), and hepatocyte growth factor (*HGF*) genes (**Supplementary Figure S1**). The RAC and SAC displayed minimal expression of insulin-like growth factor 1 (*IGF1*) and growth factors associated with neural development including nerve growth factor (*NGF*), brain-derived neurotrophic factor (*BDNF*), glial cell-derived neurotrophic factor (*GDNF*), and neuregulin 1 (*NRG1*) (**Supplementary Figure S1**). Overall, both cell populations displayed a similar gene expression profile of these paracrine factors.

Cell proliferation and survival under stress *in vitro*

The proliferation of RAC and SAC in culture was measured by a live cell imaging system every 12 hours for a period of 60 hours (**Figure 2a**). The SAC displayed a higher growth rate than the RAC (**Figure 2a**, 60 hours time point values: SAC 3.6 ± 0.4 cells normalized to initial cell number, RAC 2.4 ± 0.3, $n = 3$ populations per group; $P < 0.05$).

The cells' ability to survive conditions of oxidative and inflammatory stresses was evaluated *in vitro* with a cellular viability assay that was monitored in real-time with the live cell imaging system (**Figure 2b,c**). Under culture conditions of hydrogen peroxide-induced oxidative stress, a greater percentage of viable SAC were observed at all time points when compared with the RAC (**Figure 2b**, 72 hours time point values: SAC 48.1 ± 4.4% viability, RAC 27.7 ± 3.1%, $n = 3$ populations per group, $P < 0.05$). When exposed to inflammatory stress conditions with tumor necrosis factor-α, almost 40% of the RAC died whereas more than 85% of the SAC remained viable (**Figure 2c**, 72 hours time point values: SAC 86.1 ± 3.7% viability, RAC 61.2 ± 6.4%, $n = 2$ populations per group, $P < 0.05$). These results suggest that the SAC are more resistant to cellular death than the RAC when subjected to oxidative and inflammatory stresses, which are both likely conditions that cells will experience when injected directly into an acute MI.[19]

Intramyocardial injection and echocardiographic evaluation of cardiac function

The effect of human skeletal muscle-derived RAC and SAC for cardiac cell transplantation was assessed in an immunodeficient mouse model of an acute MI. We injected infarcted mice with cell populations isolated from three male donors ($n = 27$ mice for RAC, $n = 22$ for SAC, and $n = 21$ for control injections). The RAC

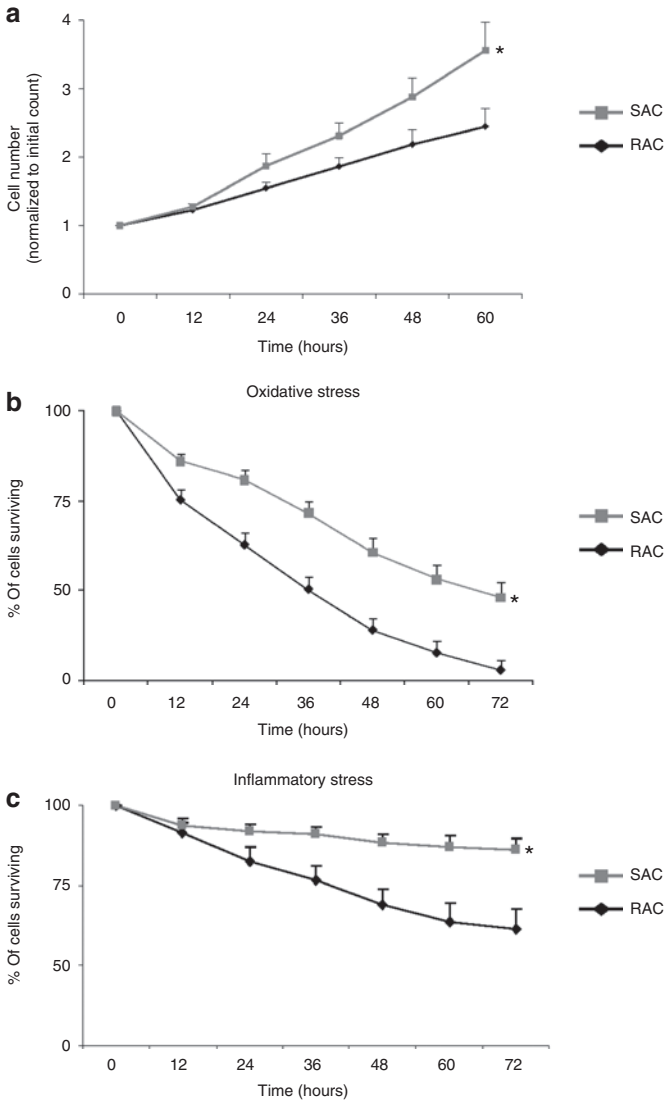

Figure 2 Cell proliferation and survival under oxidative and inflammatory stress. (**a**) Cell proliferation was measured in the RAC and SAC cultures (*$P < 0.05$). (**b**,**c**) SAC demonstrated greater survival under conditions of (**b**) oxidative and (**c**) inflammatory stress than the RAC (*$P < 0.05$). RAC, rapidly adhering cell; SAC, slowly adhering cell.

and SAC prepared for injection and frozen in cryopreservation medium displayed comparable viability and recovery post-thaw at the time of injection (post-thaw viability: RAC 89.4 ± 3.1%, SAC 89.6 ± 1.2%, $P = 0.963$; post-thaw recovery: RAC 68.4 ± 1.6%, SAC 74.9 ± 3.7%, $P = 0.189$).

Two weeks after infarction, cellular transplantation induced a modest decrease in left ventricular (LV) diastolic dimensions, as measured by end diastolic area, when compared with control vehicle injection (**Figure 3a**, SAC 11.9 ± 0.5 mm^2, RAC 12.6 ± 0.6, control 14.0 ± 0.7). Both cell groups had significantly smaller LV systolic dimensions when compared with the control group, as assessed by end systolic area (SAC 8.8 ± 0.4 mm^2, RAC 10.1 ± 0.6, control 11.9 ± 0.6; $P < 0.05$, RAC and SAC versus control). A greater improvement in LV contractility, as determined by fractional area change values, was observed in the cell-treated hearts when compared with the control vehicle-treated hearts 2 weeks after MI

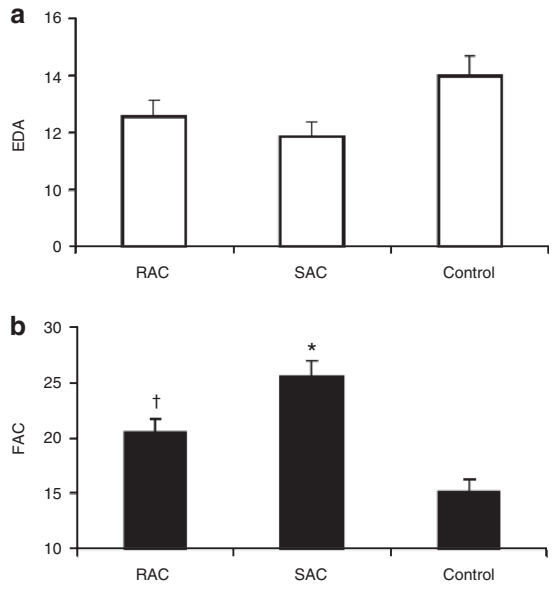

Figure 3 Functional assessments. (**a**) Left ventricular end diastolic area (EDA) was slightly reduced in hearts injected with the RAC and SAC populations when compared with control hearts injected with saline. (**b**) Hearts injected with SAC displayed stronger left ventricular contractility, as measured by percent fractional area change (FAC), when compared with hearts injected with RAC (*P < 0.05, SAC versus RAC and control; †P < 0.05, RAC versus control). RAC, rapidly adhering cell; SAC, slowly adhering cell.

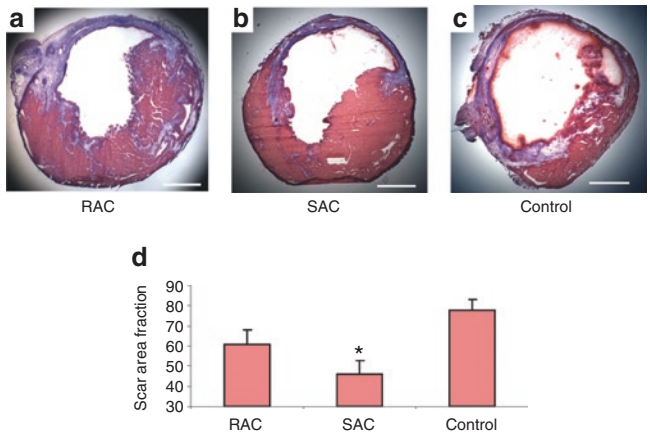

Figure 4 Infarct histology. (**a**–**c**) Representative images were taken from transverse sections of the Masson's trichrome–stained hearts. Muscle tissue is stained red, and collagenous tissue is stained blue. Bars equal 500 µm. (**d**) SAC-injected hearts demonstrated the greatest reduction of scar tissue when compared with the control (*P < 0.05, SAC versus control). RAC, rapidly adhering cell; SAC, slowly adhering cell.

(**Figure 3b**, SAC 25.6 ± 1.4%, RAC 20.6 ± 1.2%, control 15.3 ± 1.1%; P < 0.05, RAC and SAC versus control). The hearts injected with the SAC demonstrated significant improvement of LV performance when compared with the RAC (**Figure 3b**; P < 0.05, SAC versus RAC). When cardiac echocardiography data was separated by donor age, the SAC showed greater efficacy versus the RAC primarily in the older donors (57 and 70 year males) (**Supplementary Table S1**). In contrast, the SAC and RAC derived from the young donor (13-year-old male) demonstrated comparable outcomes, indicating that the selection of SAC may be the most critical from older donors (**Supplementary Table S1**). Overall, these results indicate that the SAC more effectively attenuated adverse remodeling and improved cardiac function when compared with the RAC, particularly when these cell populations were isolated from older donors.

Cardiac scar tissue

The extent of scar tissue formation within the LV was evaluated using Masson's trichrome stain (**Figure 4a–c**). Two weeks following a MI, a reduction in scar tissue was observed in both RAC- and SAC-injected hearts compared with control vehicle-injected hearts (**Figure 4d**, SAC 45.8 ± 6.6% scar, RAC 60.9 ± 7.1%, control 77.5 ± 5.3%). However, only the SAC significantly attenuated scar tissue formation following an acute MI when compared with the controls (**Figure 4d**, P < 0.05, SAC versus control).

Transplanted cell engraftment and proliferation

Donor myocytes were observed within the infarct zone by colocalization of Masson's trichrome stain (arrows, **Figure 5a**) and fast skeletal MYH immunostaining (arrows, **Figure 5b**). These engraftments were frequently surrounded by scar tissue along the ischemic border zone (arrowheads, **Figure 5a,b**). The area of MYH$^+$ tissue within the myocardium of the LV was comparable between hearts injected with the RAC and SAC (SAC 3.5 ± 1.2% MYH$^+$ tissue in the myocardium, RAC 3.8 ± 0.8%, P = 0.864, SAC versus RAC). The presence of nuclei expressing proliferating cell nuclear antigen (PCNA) using a human-specific PCNA antibody further confirmed donor cell engraftment and indicated donor cell proliferation *in vivo* (**Figure 5c**). We observed proliferative, PCNA-positive donor cells more frequently in the SAC-injected hearts than in the RAC-injected hearts (**Figure 5d**, SAC 2.0 ± 0.3 PCNA$^+$/MYH$^+$ cells, RAC 0.4 ± 0.3; P < 0.05, SAC versus RAC). These findings confirm the engraftment of the injected human cells within the murine myocardium, and suggest that the SAC proliferate at higher levels than the RAC *in vivo*.

Angiogenesis

Capillary density within the infarct tissue was assessed by CD31 immunostaining (**Figure 6a–c**). More capillaries were observed within the infarct area of hearts treated with the SAC when compared with hearts injected with the RAC and the control vehicle (**Figure 6d**, SAC 723 ± 63 capillaries/mm^2, RAC 560 ± 21, control 548 ± 31; P < 0.05, SAC versus RAC and control). These findings indicate that transplanted SAC may induce a more potent angiogenic effect within the infarcted hearts when compared with transplanted RAC and the control.

Endogenous cardiomyocyte apoptosis and proliferation

Endogenous cardiomyocyte apoptosis and proliferation was evaluated at 3 days after MI. Multi-label staining for terminal dUPT nick end-labeling (TUNEL) and cardiac Troponin I (cTnI) was performed to determine the effect of cell implantation on endogenous cardiomyocyte apoptosis in the peri-infarct regions (**Figure 7a**). Hearts injected with SAC contained less apoptotic cardiomyocytes within the peri-infarct regions when compared with hearts transplanted with RAC and the control vehicle (**Figure 7b**, SAC 203 ± 29

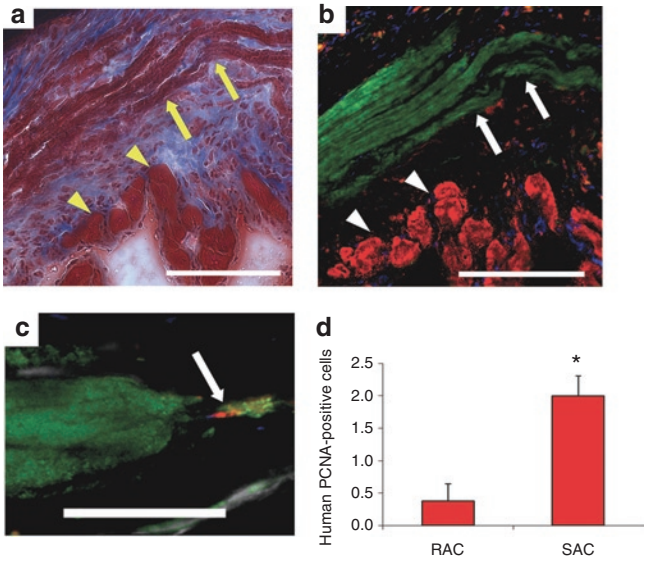

Figure 5 Engraftment and proliferation of injected cells *in vivo*. (**a**) The arrows designate the engraftment area of the SAC, and the arrowheads indicate host cardiac tissue in Masson's trichrome–stained hearts. Bar equals 125 µm. Image **a** colocalizes with image **b**. (**b**) Fast skeletal myosin heavy chain (MYH)-positive myofibers (green stain, arrows) designate the SAC engraftment region. Cardiac troponin I-positive cardiomyocytes (red, arrowheads) identifies peri-infarct zone. Bar equals 125 µm. (**c**,**d**) Mitotic human PCNA-positive cells (red stain) that colocalized with the MYH-positive engraftment region (green stain) were more frequently observed in the SAC-injected hearts when compared with the RAC-injected hearts (*$P < 0.05$, SAC versus RAC). Cardiac troponin I-positive cardiomyocytes are stained grey, and nuclei are stained blue. PCNA, proliferating cell nuclear antigen; RAC, rapidly adhering cell; SAC, slowly adhering cell.

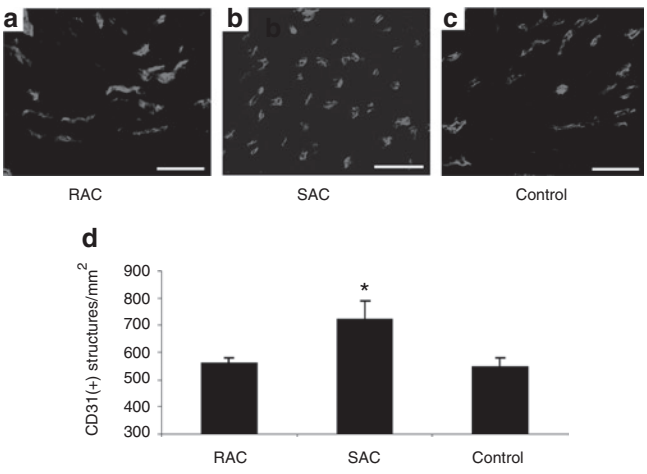

Figure 6 Angiogenesis. (**a**–**c**) Representative images are shown of CD31 immunostaining. Bars equal 50 µm. (**d**) The infarcts of hearts transplanted with SAC displayed higher capillary densities when compared with hearts injected with RAC and control vehicle (*$P < 0.05$, SAC versus RAC and control). RAC, rapidly adhering cell; SAC, slowly adhering cell.

TUNEL$^+$/cTnI$^+$ cells in four high power fields, RAC 321 ± 68, control 404 ± 81; $P < 0.05$, SAC versus control).

The number of proliferating cardiomyocytes present within the infarct border zone was measured by Ki-67 and cTnI dual label immunostaining (**Figure 7c**). Hearts injected with SAC contained more proliferating cardiomyocytes within the infarct border zone

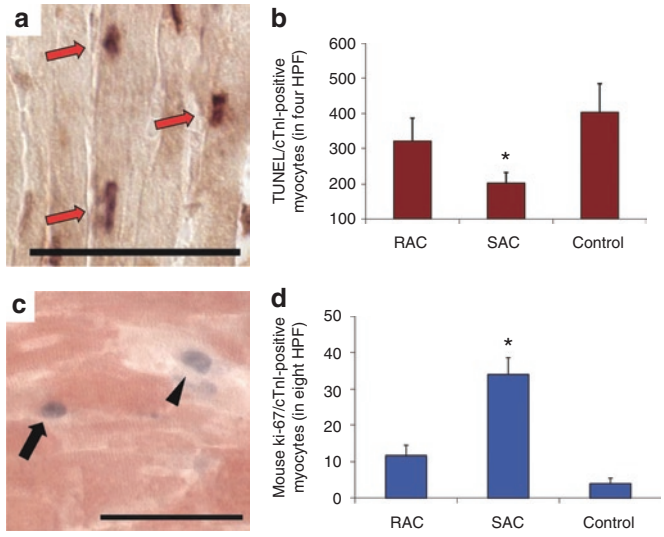

Figure 7 Endogenous cardiomyocyte apoptosis and proliferation. (**a**) Identification of apoptotic endogenous cardiomyocytes (arrows) by concomitant staining for cardiac troponin I (cTnI, light brown cytoplasmic stain) and TUNEL assay (arrows, dark nuclear stain). Bar equals 50 µm. (**b**) The number of apoptotic cardiomyocytes was measured in four high power fields (HPF, *$P < 0.05$, SAC versus control). (**c**) Proliferating cardiomyocytes (arrow) within the peri-infarct region were identified by colocalization of both Ki-67 (blue nuclear stain) and cTnI (red) within the peri-infarct region. Some of the proliferating cells stained by Ki-67 did not colocalize with cTnI (arrowhead). Bar equals 50 µm. (**d**) The number of proliferating Ki-67-positive endogenous cardiomyocytes was measured in the peri-infarct region of the hearts (*$P < 0.05$, SAC versus RAC and control). HPF, high power field; RAC, rapidly adhering cell; SAC, slowly adhering cell, TUNEL, terminal dUPT nick end-labeling.

than hearts injected with either the RAC or the control (**Figure 7d**, SAC 34 ± 5 Ki-67$^+$/cTnI$^+$ cardiomyocytes in 8 high power fields, RAC 12 ± 3, control 4 ± 2; $P < 0.05$, SAC versus RAC and control). Taken together, these results suggest that the transplantation of SAC induced a beneficial effect on endogenous cardiomyocyte proliferation and apoptosis within the peri-infarct region.

DISCUSSION

The main finding in this study is that the SAC fraction is more effective at improving cardiac function than the RAC fraction derived from human skeletal muscle, which is a result that is consistent with our studies investigating progenitor cells from murine skeletal muscle for cardiac repair.[16] These results support the notion that human skeletal muscle-derived progenitor cells are heterogeneous not just in terms of cellular composition but of potency for cardiac cell transplantation.

Isolation of human skeletal muscle-derived cells on the basis of adhesion rates to tissue culture flasks using the preplate technique produced RAC and SAC populations that exhibit distinct characteristics and behavior. Our results *in vitro* demonstrate that myogenic progenitor cells with the highest myogenic purity and the strongest propensity for myogenic differentiation are purified in the SAC fraction rather than the RAC fraction. Interestingly, these findings in human skeletal muscle are consistent with the use of the preplate technique to isolate progenitor cells from murine skeletal muscle.[14] In the mouse, we observed that cells that adhered slowly also displayed greater myogenic purity based on DES

expression when compared with cells that adhered rapidly.[14] In addition, the murine SAC population displayed a greater ability to regenerate skeletal muscle than the RAC population.[14] The mechanism underlying differential adhesion rates to tissue culture flasks is unknown at this point; however, these differences may result from a variety of factors including the expression of specific adhesion molecules and cellular density.[17] We are initiating research to determine whether other human skeletal muscle-derived cell populations, including $CD34^{+}CD90^{-}$ cells,[5] myogenic endothelial cells[12,13] and pericytes,[10,11] are being collected preferentially in the slowly adhering fraction. Due to the limited number of cells (<100) contained within the slowly adhering fraction before expansion, and the known change in expression of many surface markers with time *in vitro*, flow cytometry characterization with a series of cell surface markers on the same populations used in this study for injection was not achievable.

The mechanism underlying the advantage of the SAC over RAC population for functional restoration after a MI may be multi-faceted.[7,16,20–25] A proposed aspect for the observed functional difference might be the varying ability of the transplanted cells to prevent adverse remodeling. SAC-treated hearts displayed a considerable reduction in end-systolic geometry when compared with RAC-injected hearts, suggesting that SAC induced a more effective attenuation of adverse remodeling. In clinical trials, skeletal myoblasts have shown a positive remodeling effect in the first randomized, placebo-controlled study of skeletal myoblast transplantation for cardiac repair (MAGIC trial).[26] The observed differences in end-systolic dimensions between the SAC and RAC could be attributed to the greater reduction in scar tissue in SAC-treated hearts when compared with hearts treated with RAC.

The reduced size of the infarct scar may be due to the preservation of at-risk cardiomyocytes, stimulation of endogenous cardiomyocyte proliferation, vascularization of the infarct scar, and/or the secretion of paracrine factors that regulate fibrosis. Three days after MI, we observed a significant increase in the number of proliferating cardiomyocytes and decrease in the number of apoptotic cardiomyocytes within the peri-infarct zone of hearts injected with SAC when compared with hearts injected with RAC and the control vehicle. We did not determine how the injected cells stimulated proliferation and protection of at-risk myocardium; however, at such an early time point after MI (3 days), a reasonable hypothesis is that this effect is due to the release of paracrine factors by the injected cells that stimulate cell survival and proliferation. Furthermore, various reports have shown that implanted cells promote infarct angiogenesis and have established a correlation between neovascularization and functional recovery of the heart after MI.[13,16,27,28] Here, we also observed a greater induction of angiogenesis within the infarct in SAC-treated hearts than in RAC-treated hearts, which may also support the attenuation of adverse infarct remodeling.[26,29]

The cells' ability to influence the host cells within the microenvironment through the release of paracrine molecules may represent a major determinant in the healing capacity of transplanted cells.[30,31] Here, we showed that both RAC and SAC express similar levels of various angiogenic and neurogenic genes under normal culture conditions. Many of the angiogenic factors expressed by the RAC and SAC, especially *VEGFA*, *HGF*, *TGFB1*, and *FGF2*, have been shown to be expressed by human skeletal myoblasts, bone marrow mononuclear cells, adipose stromal cells, and bone marrow stromal cells.[32–37] In addition to stimulating angiogenesis, factors secreted by transplanted cells may activate signaling cascades that regulate fibrosis and the survival and proliferation of recipient cells in and around the infarct zone. Human skeletal muscle-derived cells likely express a wide variety of paracrine factors that far surpass the small battery of genes evaluated by others and us.[32,33] It is not unexpected that both the RAC and SAC populations express similar levels of the tested paracrine factors under normal culture conditions, since the level of cellular secretion of these factors may be primarily dependent on the cells' response to the environmental cues of the myocardial microenvironment and disease state (e.g., ischemia).[13,16,27,28]

Furthermore, the magnitude of the paracrine effect may be contingent on cell survival post-transplantation. The ability of transplanted cells to survive and proliferate, particularly when implanted directly into the harsh *milieu* of a myocardial infarct, may be critical for the cells to exert a lasting and significant biological effect, including the extended release of paracrine factors.[19] In our research with muscle progenitor cells isolated from human and murine skeletal muscle, we have consistently observed that transplanted SAC regenerate larger and more durable engraftments of skeletal myocytes than transplanted RAC.[14–16] We hypothesize that the preplate technique inherently selects for stress-resistant cells in the slowly adhering fraction, since these cells are able to tolerate suspension-induced stresses and anoikis during isolation.[38,39] Therefore, the SAC may represent a cell population endowed with an elevated resistance to stress. We have recently shown that muscle stem cells derived from the SAC fraction of murine skeletal muscle have an ability to survive under stress due to elevated levels of antioxidant expression.[40,41] Future research will evaluate whether human SAC also display similar antioxidant characteristics.

A limitation of this study is of the fact that the skeletal muscle-derived cells were injected immediately after a MI, which is not entirely relevant to an actual clinical scenario for autologous transplantation. In reality, the cells would require at least several weeks in order to cultivate a sufficient number of cells before treatment. Although we could not replicate the exact clinical conditions with this animal model, these findings may still provide meaningful information regarding the heterogeneity of human skeletal muscle-derived cells for cardiac cell transplantation.

In conclusion, the isolation of adult human skeletal muscle-derived cells on the basis of adhesion rates to tissue culture flasks enriches for cell fractions that support distinct levels of functional improvement when transplanted into ischemic myocardium. Selection of the best progenitor cell population from human skeletal muscle may aid in the translation of cell-based products for clinical applications of tissue repair.

MATERIALS AND METHODS

Animals. The Institutional Animal Care and Use Committee at the Children's Hospital of Pittsburgh approved the animal and surgical procedures performed in this study (Protocol 37/04). A total of 70 male nonobese diabetic/severe combined immunodeficient mice (NOD/SCID, strain NOD.CB17-*Prkdc*^{scid}/SzJ, The Jackson Laboratory, Bar Harbor, ME) between

13 and 22 weeks of age were used for this study. Creation of the acute MI model in adult mice and injection of thawed cells (3×10^5 cells in 30 µl) or control medium (30 µl) was performed in a blinded fashion, as previously described.[16] Echocardiography was also conducted in a blinded fashion to assess heart function, as previously described.[13,16] Additional information can be found in the **Supplementary Materials and Methods**.

Cells. RAC and SAC populations were isolated from human rectus abdominus skeletal muscle biopsies (50–250 mg) using the preplate technique.[17] Tissues were procured from 13, 57, and 70-year-old male donors (13M, 57M, and 70M, respectively). Isolation, culture expansion, and preparation of cells for injection are further detailed in **Supplementary Materials and Methods**. Cell populations from each donor were cryopreserved for injection at the following culture passages: 13M–RAC passage 4 and SAC passage 5–7, 57M–RAC passage 6 and SAC passage 5, 70M–RAC passage 8 and SAC passage 7. Post-thaw recovery and viability were evaluated from aliquots of the frozen cell suspensions that were prepared and cryopreserved for injection using the Viacount viability stain (Millipore, Hayward, CA) and Guava PCA flow cytometry system (Millipore).

Gene expression profile. RNA was purified from 1×10^5 cells for gene expression analysis immediately following the thaw of the cryopreserved stocks of cultured cells. The number of passages of the RAC and SAC were closely matched for the populations derived from the 13M (passage 7 for RAC and passage 6 for SAC), 57M (passage 6 for both populations), and 70M donor tissues (passage 3 for both populations).

Total RNA was isolated using the RNeasy Mini kit (Qiagen, Valencia, CA) and was reverse transcribed to cDNA (Applied Biosystems, Foster City, CA). Gene expression was measured using real-time quantitative PCR (see **Supplementary Materials and Methods** for detailed methods). All target genes were normalized to the reference housekeeping gene *IPO8* (Applied Biosystems, Hs00183533_m1). Relative quantity of gene expression was calculated as total amount of RNA based on the comparative ΔC_T (cycle threshold) (*i.e.*, relative expression level to endogenous control gene *IPO8*) and $\Delta\Delta C_T$ methods (i.e., relative expression level to the RAC population for each donor).

Myogenic assays. Myogenic purity analysis was performed on cellular suspensions using a PE-conjugated CD56 antibody (1:50; BD Pharmingen, San Diego, CA). The Guava PCA flow cytometry system measured the percentage of cells expressing CD56. Cell populations from each donor were evaluated at the following culture passages: 13M–RAC passage 4 and SAC passage 5–7, 57M–RAC passage 6 and SAC passage 5, 70M–RAC passage 8 and SAC passage 7.

To determine the myogenic differentiation potential of each population, cells were seeded onto a culture plate with low-serum differentiation medium and allowed to differentiate. Cell populations from each donor were evaluated at the following culture passages: 13M–RAC passage 4–5 and SAC passage 6–7, 57M–RAC passage 6 and SAC passage 5, 70M–RAC passage 4 and SAC passage 4. Terminal differentiation into multi-nucleated myotubes was measured with an assay that measured creatine kinase (CK) activity levels of differentiated cultures using the CK Liqui-UV Test Kit (Stanbio Laboratory, Boerne, TX) according to the manufacturer's instructions.[42]

Cell proliferation and survival assays. Cell proliferation under normal culture conditions and cell viability under stress conditions were evaluated with kinetic assays.[12,40,41] Cells were cultured for 60 hours in a live cell imaging system (Automated Cell, Pittsburgh, PA), which contains an incubation chamber for controlling temperature, humidity and CO_2 gas levels. The number of cells was measured in images acquired at 12-hour intervals.

Cell viability under stress conditions was analyzed as previously described.[12,40,41] Briefly, cells were cultured in a live cell imaging system for 72 hours in medium supplemented with propidium iodide (1:500, Sigma, St Louis, MO) to stain dead cells and either hydrogen peroxide (300 µmol/l; Sigma) or tumor necrosis factor-α (10 ng/ml; Sigma) to induce cell death by oxidative and inflammatory stresses, respectively. Brightfield and fluorescent images were captured repeatedly at 10-minute intervals in the live cell imaging system for the entire 72-hour period. The percentage of viable cells (*i.e.*, propidium iodide exclusion) was measured from images acquired at 12-hour intervals using imaging software.

Histology and immunohistochemistry. Mice were sacrificed at 3 days, 2 weeks or 6 weeks after cell transplantation. We harvested the hearts, froze the tissue in 2-methylbutane precooled in liquid nitrogen, and serially sectioned the hearts from the apex to the base, as previously described.[13] Sections were then stained for fast skeletal MYH (1:200–1:400; Sigma) expression, as previously described.[20] The engraftment area ratio was defined as the area of MYH-positive tissue divided by the total area of the LV myocardium, which was identified by co-staining for cTnI (1:20,000; Scripps Laboratories, San Diego, CA). To detect proliferating cells within the engraftment, tissue was stained with human anti-human PCNA antibody (1:400; US Biological, Swampscott, MA).[13] In sections stained with Masson's trichrome (IMEB, San Marcos, CA), scar area fraction was defined as the ratio of scar area to the cardiac LV muscle area and was averaged from five sections per heart, as previously described.[13] To measure capillary density, we stained heart muscle sections with an anti-mouse CD31 (platelet/endothelial cell adhesion molecule-1) antibody (BD Pharmingen).[16] The TUNEL assay was performed using the ApopTag Plus Peroxidase In Situ Apoptosis Detection Kit (Chemicon, Temecula, CA) according to manufacturer's instructions.[13] We carried out the Ki-67 (1:50; Dako, Glostrup, Denmark) and cTnI dual label immunostaining, as previously described, using the SG substrate kit (blue stain, Vector Laboratories, Burlingame, CA) and the AEC (3-amino-9-ethylcarbazole) substrate kit (red stain, Vector Laboratories), respectively.[13] Additional immunostaining methods are provided in the **Supplementary Materials and Methods**.

Statistical analysis. All measured data are presented as the mean ± SE of the mean. A *t*-test or a one-way analysis of variance was performed when comparing two groups or more than two groups, respectively. Analysis of variance *post hoc* analysis was conducted with the Tukey multiple comparison test. Statistical significance was defined by a value of $P < 0.05$. All calculations were performed using SigmaStat (Systat Software, San Jose, CA).

SUPPLEMENTARY MATERIAL

Figure S1. Cytokine gene expression profile.
Table S1. Echocardiographic data separated by donor cell populations.
Materials and Methods.

ACKNOWLEDGMENTS

The authors would like to thank Theresa Casino, Burhan Gharaibeh, and Jessica Tebbets for their technical assistance and James Cummins for his editorial assistance with the manuscript. This work was supported, in part, by grants from Cook MyoSite Inc., the National Institutes of Health (5U54AR050733-06), the Donaldson Chair at Children's Hospital of Pittsburgh, and the Mankin Chair at the University of Pittsburgh. The authors wish to disclose that J.H. has a potential financial conflict of interest because he has received remuneration as a consultant with Cook MyoSite Inc. The authors also wish to disclose that T.P. and R.J.J. are employees of Cook MyoSite, Inc. and that the work was partly funded by Cook MyoSite Incorporated. The other authors declared no conflict of interest.

REFERENCES

1. Péault, B, Rudnicki, M, Torrente, Y, Cossu, G, Tremblay, JP, Partridge, T *et al.* (2007). Stem and progenitor cells in skeletal muscle development, maintenance, and therapy. *Mol Ther* **15**: 867–877.
2. Menasché, P (2004). Cellular transplantation: hurdles remaining before widespread clinical use. *Curr Opin Cardiol* **19**: 154–161.
3. Huard, J, Acsadi, G, Jani, A, Massie, B and Karpati, G (1994). Gene transfer into skeletal muscles by isogenic myoblasts. *Hum Gene Ther* **5**: 949–958.

4. Beauchamp, JR, Morgan, JE, Pagel, CN and Partridge, TA (1999). Dynamics of myoblast transplantation reveal a discrete minority of precursors with stem cell-like properties as the myogenic source. *J Cell Biol* **144**: 1113–1122.
5. Proksch, S, Bel, A, Puymirat, E, Pidial, L, Bellamy, V, Peyrard, S *et al.* (2009). Does the human skeletal muscle harbor the murine equivalents of cardiac precursor cells? *Mol Ther* **17**: 733–741.
6. Negroni, E, Riederer, I, Chaouch, S, Belicchi, M, Razini, P, Di Santo, J *et al.* (2009). *In vivo* myogenic potential of human CD133+ muscle-derived stem cells: a quantitative study. *Mol Ther* **17**: 1771–1778.
7. Sarig, R, Baruchi, Z, Fuchs, O, Nudel, U and Yaffe, D (2006). Regeneration and transdifferentiation potential of muscle-derived stem cells propagated as myospheres. *Stem Cells* **24**: 1769–1778.
8. Morosetti, R, Mirabella, M, Gliubizzi, C, Broccolini, A, Sancricca, C, Pescatori, M *et al.* (2007). Isolation and characterization of mesoangioblasts from facioscapulohumeral muscular dystrophy muscle biopsies. *Stem Cells* **25**: 3173–3182.
9. Motohashi, N, Uezumi, A, Yada, E, Fukada, S, Fukushima, K, Imaizumi, K *et al.* (2008). Muscle CD31(-) CD45(-) side population cells promote muscle regeneration by stimulating proliferation and migration of myoblasts. *Am J Pathol* **173**: 781–791.
10. Dellavalle, A, Sampaolesi, M, Tonlorenzi, R, Tagliafico, E, Sacchetti, B, Perani, L *et al.* (2007). Pericytes of human skeletal muscle are myogenic precursors distinct from satellite cells. *Nat Cell Biol* **9**: 255–267.
11. Crisan, M, Yap, S, Casteilla, L, Chen, CW, Corselli, M, Park, TS *et al.* (2008). A perivascular origin for mesenchymal stem cells in multiple human organs. *Cell Stem Cell* **3**: 301–313.
12. Zheng, B, Cao, B, Crisan, M, Sun, B, Li, G, Logar, A *et al.* (2007). Prospective identification of myogenic endothelial cells in human skeletal muscle. *Nat Biotechnol* **25**: 1025–1034.
13. Okada, M, Payne, TR, Zheng, B, Oshima, H, Momoi, N, Tobita, K *et al.* (2008). Myogenic endothelial cells purified from human skeletal muscle improve cardiac function after transplantation into infarcted myocardium. *J Am Coll Cardiol* **52**: 1869–1880.
14. Qu, Z, Balkir, L, van Deutekom, JC, Robbins, PD, Pruchnic, R and Huard, J (1998). Development of approaches to improve cell survival in myoblast transfer therapy. *J Cell Biol* **142**: 1257–1267.
15. Qu-Petersen, Z, Deasy, B, Jankowski, R, Ikezawa, M, Cummins, J, Pruchnic, R *et al.* (2002). Identification of a novel population of muscle stem cells in mice: potential for muscle regeneration. *J Cell Biol* **157**: 851–864.
16. Oshima, H, Payne, TR, Urish, KL, Sakai, T, Ling, Y, Gharaibeh, B *et al.* (2005). Differential myocardial infarct repair with muscle stem cells compared to myoblasts. *Mol Ther* **12**: 1130–1141.
17. Gharaibeh, B, Lu, A, Tebbets, J, Zheng, B, Feduska, J, Crisan, M *et al.* (2008). Isolation of a slowly adhering cell fraction containing stem cells from murine skeletal muscle by the preplate technique. *Nat Protoc* **3**: 1501–1509.
18. Pilling, D, Fan, T, Huang, D, Kaul, B and Gomer, RH (2009). Identification of markers that distinguish monocyte-derived fibrocytes from monocytes, macrophages, and fibroblasts. *PLoS ONE* **4**: e7475.
19. Suzuki, K, Murtuza, B, Beauchamp, JR, Smolenski, RT, Varela-Carver, A, Fukushima, S *et al.* (2004). Dynamics and mediators of acute graft attrition after myoblast transplantation to the heart. *FASEB J* **18**: 1153–1155.
20. Payne, TR, Oshima, H, Sakai, T, Ling, Y, Gharaibeh, B, Cummins, J *et al.* (2005). Regeneration of dystrophin-expressing myocytes in the mdx heart by skeletal muscle stem cells. *Gene Ther* **12**: 1264–1274.
21. Reinecke, H, Poppa, V and Murry, CE (2002). Skeletal muscle stem cells do not transdifferentiate into cardiomyocytes after cardiac grafting. *J Mol Cell Cardiol* **34**: 241–249.
22. Reinecke, H, Minami, E, Poppa, V and Murry, CE (2004). Evidence for fusion between cardiac and skeletal muscle cells. *Circ Res* **94**: e56–e60.
23. Reinecke, H, MacDonald, GH, Hauschka, SD and Murry, CE (2000). Electromechanical coupling between skeletal and cardiac muscle. Implications for infarct repair. *J Cell Biol* **149**: 731–740.
24. Leobon, B, Garcin, I, Menasche, P, Vilquin, JT, Audinat, E and Charpak, S (2003). Myoblasts transplanted into rat infarcted myocardium are functionally isolated from their host. *Proc Natl Acad Sci USA* **100**: 7808–7811.
25. Rubart, M, Soonpaa, MH, Nakajima, H and Field, LJ (2004). Spontaneous and evoked intracellular calcium transients in donor-derived myocytes following intracardiac myoblast transplantation. *J Clin Invest* **114**: 775–783.
26. Menasché, P, Alfieri, O, Janssens, S, McKenna, W, Reichenspurner, H, Trinquart, L *et al.* (2008). The Myoblast Autologous Grafting in Ischemic Cardiomyopathy (MAGIC) trial: first randomized placebo-controlled study of myoblast transplantation. *Circulation* **117**: 1189–1200.
27. Kocher, AA, Schuster, MD, Szabolcs, MJ, Takuma, S, Burkhoff, D, Wang, J *et al.* (2001). Neovascularization of ischemic myocardium by human bone-marrow-derived angioblasts prevents cardiomyocyte apoptosis, reduces remodeling and improves cardiac function. *Nat Med* **7**: 430–436.
28. Payne, TR, Oshima, H, Okada, M, Momoi, N, Tobita, K, Keller, BB *et al.* (2007). A relationship between vascular endothelial growth factor, angiogenesis, and cardiac repair after muscle stem cell transplantation into ischemic hearts. *J Am Coll Cardiol* **50**: 1677–1684.
29. White, HD, Norris, RM, Brown, MA, Brandt, PW, Whitlock, RM and Wild, CJ (1987). Left ventricular end-systolic volume as the major determinant of survival after recovery from myocardial infarction. *Circulation* **76**: 44–51.
30. Gnecchi, M, Zhang, Z, Ni, A and Dzau, VJ (2008). Paracrine mechanisms in adult stem cell signaling and therapy. *Circ Res* **103**: 1204–1219.
31. Cheng, AS and Yau, TM (2008). Paracrine effects of cell transplantation: strategies to augment the efficacy of cell therapies. *Semin Thorac Cardiovasc Surg* **20**: 94–101.
32. Perez-Ilzarbe, M, Agbulut, O, Pelacho, B, Ciorba, C, San Jose-Eneriz, E, Desnos, M *et al.* (2008). Characterization of the paracrine effects of human skeletal myoblasts transplanted in infarcted myocardium. *Eur J Heart Fail* **10**: 1065–1072.
33. Ebelt, H, Jungblut, M, Zhang, Y, Kubin, T, Kostin, S, Technau, A *et al.* (2007). Cellular cardiomyoplasty: improvement of left ventricular function correlates with the release of cardioactive cytokines. *Stem Cells* **25**: 236–244.
34. Kinnaird, T, Stabile, E, Burnett, MS, Shou, M, Lee, CW, Barr, S *et al.* (2004). Local delivery of marrow-derived stromal cells augments collateral perfusion through paracrine mechanisms. *Circulation* **109**: 1543–1549.
35. Kinnaird, T, Stabile, E, Burnett, MS, Lee, CW, Barr, S, Fuchs, S *et al.* (2004). Marrow-derived stromal cells express genes encoding a broad spectrum of arteriogenic cytokines and promote *in vitro* and *in vivo* arteriogenesis through paracrine mechanisms. *Circ Res* **94**: 678–685.
36. Tse, HF, Siu, CW, Zhu, SG, Songyan, L, Zhang, QY, Lai, WH *et al.* (2007). Paracrine effects of direct intramyocardial implantation of bone marrow derived cells to enhance neovascularization in chronic ischaemic myocardium. *Eur J Heart Fail* **9**: 747–753.
37. Rehman, J, Traktuev, D, Li, J, Merfeld-Clauss, S, Temm-Grove, CJ, Bovenkerk, JE *et al.* (2004). Secretion of angiogenic and antiapoptotic factors by human adipose stromal cells. *Circulation* **109**: 1292–1298.
38. Feng, J, Yang, S, Xu, L, Tian, H, Sun, L and Tang, X (2007). Role of caspase-3 inhibitor in induced anoikis of mesenchymal stem cells in vitro. *J Huazhong Univ Sci Technol Med Sci* **27**: 183–185.
39. Luebke-Wheeler, JL, Nedredal, G, Yee, L, Amiot, BP and Nyberg, SL (2009). E-cadherin protects primary hepatocyte spheroids from cell death by a caspase-independent mechanism. *Cell Transplant* **18**: 1281–1287.
40. Urish, KL, Vella, JB, Okada, M, Deasy, BM, Tobita, K, Keller, BB *et al.* (2009). Antioxidant levels represent a major determinant in the regenerative capacity of muscle stem cells. *Mol Biol Cell* **20**: 509–520.
41. Drowley, L, Okada, M, Beckman, S, Vella, J, Keller, B, Tobita, K *et al.* (2010). Cellular antioxidant levels influence muscle stem cell therapy. *Mol Ther* **18**: 1865–1873.
42. Kumar, A, Mohan, S, Newton, J, Rehage, M, Tran, K, Baylink, DJ *et al.* (2005). Pregnancy-associated plasma protein-A regulates myoblast proliferation and differentiation through an insulin-like growth factor-dependent mechanism. *J Biol Chem* **280**: 37782–37789.